

## Spectroelectrochemical and Theoretical Tools Applied towards an Enhanced Understanding of Structure, Energetics and Dynamics of Molecules and Polymers: Polyfuranes, Polythiophenes, Polypyrroles and their Copolymers\*

J. Arjomandi<sup>†</sup>, F. Alakhras, W. Al-Halasa<sup>‡</sup> and R. Holze<sup>‡</sup>

Institut für Chemie, Technische Universität Chemnitz, AG Elektrochemie, D-09107 Chemnitz, Germany

Received on April 23, 2009

Accepted on Aug. 28, 2009

### Abstract

A brief selective, introductory overview of applications of non-classical, in particular spectroelectrochemical and theoretical, methods, to various challenges from interfacial and materials electrochemistry as well as electrochemical and chemical kinetics and thermodynamics is provided including representative illustrating examples with particular attention to intrinsically conducting polymers. Going beyond previously well established applications of spectroscopic methods in determination of molecular structure (in particular vibrational spectroscopies) and electrooptical properties (UV-Vis spectroscopy) thermodynamic data (formal redox potentials, oxidation and reduction potentials of monomer and polymer transformations) and supramolecular interactions are studied with various spectroscopic methods combined with theoretical tools like density functional theory and *ab initio* calculations. Selected examples particularly useful to illustrate these possibilities from recent studies of polythiophenes, polyfurans, polypyrroles and their respective copolymers are briefly reviewed.

**Keywords:** Intrinsically conducting polymer; Electrochemistry; Spectroelectrochemistry; Density functional theory.

### Introduction

Electrochemistry as known to most chemists deals with numerous rather different subjects ranging from energy storage and conversion over analytical methods, synthetic procedures, surface treatment, and corrosion up to bioelectrochemistry and beyond. Because of the extreme width of subjects and the sometimes rather specialized applications well established in areas far away from traditional electrochemistry the overall picture and with it the more fundamental capabilities of electrochemistry tend to be overlooked. The still growing interest of inorganic, bioinorganic and organic chemists in electrochemical methods and models indicates a considerable interest in these capabilities, but in most cases of applications the true potential of electrochemistry is not exhausted at all.

\* Paper presented at the Petra International Chemistry Conference, Petra, Jordan, 2007

† Current address: Faculty of Chemistry, Buai Sina University, 65178 Hamedan, Iran

‡ To whom correspondence should be addressed. E-mail: rudolf.holze@chemie.tu-chemnitz.de

Investigations of the structure of electrochemical interfaces, i.e. in the most basic case the phase boundary between e.g. a solid metal and an aqueous electrolyte solution, have been limited for a long time to the application of traditional electrochemical methods wherein voltage/potential, current, charge and some other experimental variables like temperature, concentration or pressure were either measured or varied. Results of these methods pertaining e.g. to Gibbs energy of adsorption  $\Delta G_{ad}$  or electrode potential of zero charge  $E_{pzc}$  are numerous and valuable <sup>[1]</sup>. A microscopic picture of the interface emerged only more recently. Based on the application of numerous spectroscopic and surface science methods details of the interface at the atomic and molecular level could be elucidated. Numerous probes can be applied in methods mostly derived from surface science and analytical chemistry yielding various signals as symbolically illustrated in figure 1: Electromagnetic radiation ( $h \cdot \nu$ ), neutral atom beams ( $i^0$ ), ion beams ( $i^\pm$ ), magnetic (H) or electric (E) fields and thermal excitation (W) can be used as probes or probe-like; upon interaction with the surface or interface respective signals can be observed. Obviously several methods cannot be applied *in situ*, i.e. in the presence of an electrolyte solution or a liquid electrolyte (molten salt, ionic liquid or deep eutectic). This mode of operation is preferable because it avoids artifacts possibly caused by the transfer of the sample under investigation from e.g. an electrochemical cell into an ultrahigh vacuum chamber. Even for those vacuum-based methods approaches limiting the possible errors have been developed. Nevertheless already those methods which employ probes and signals which can be applied *in situ* are numerous <sup>[2]</sup>. Beyond the methods now generally called spectroelectrochemical ones surface-analytical methods like e.g. scanning probe microscopies, confocal methods or surface conductivity measurements have been adapted successfully.

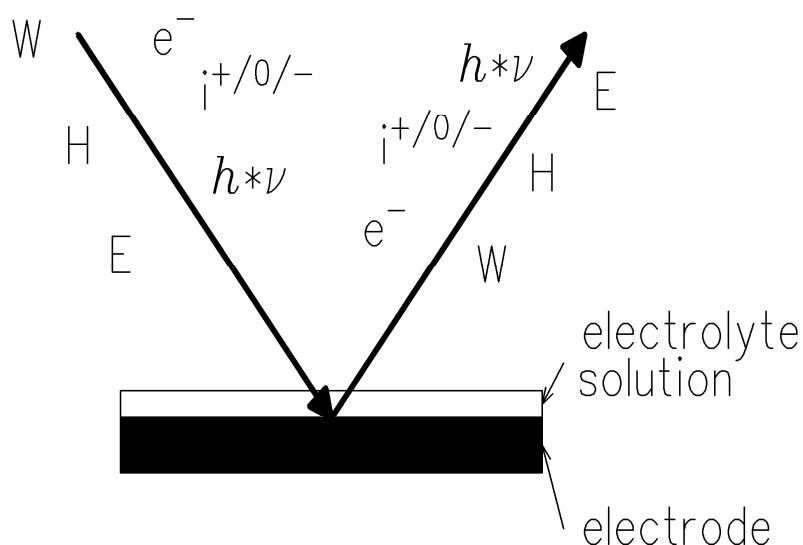


**Figure 1:** Probes and signals in spectroelectrochemistry, for meaning of symbols see text.

In this brief report selected possibilities of electrochemistry and in particular spectroelectrochemistry and surface analytical methods <sup>[2]</sup> as applied to several challenging questions related to intrinsically conducting polymers as a rather new and particularly challenging class of materials are highlighted, for a thorough discussion, complete deduction of mathematical formulation etc. the reader might wish to consult the original papers published elsewhere and quoted in the references.

Polymeric materials both of inorganic as well as organic origin are generally insulating substances. Since the surprising discovery of the unusual electrooptical properties of polyacetylene by Shirakawa et al. <sup>[3, 4]</sup> and the subsequent development of electrochemical methods for formation, modification and characterization of these materials subsequently called intrinsically conducting polymers (ICPs, also synthetic metals) by Diaz et al. <sup>[5]</sup> this class of materials has shown an explosive development regarding the scope of investigated monomers, methods of polymerization and characterization and suggested applications. Numerous reviews covering selected members of the family are available <sup>[6]</sup>. Most applications of electrochemical, in particular spectroelectrochemical methods, have aimed at elucidating molecular-structural features and electrooptical properties. Use of theoretical methods in understanding or even predicting properties as pioneered by Bredas et al. in their studies of polypyrrole <sup>[7]</sup> has seen wide application recently because of availability of various computational tools manageable even by non-experts. Beyond structural properties derived from e.g. the comparison of measured and calculated vibrational spectra results of both *ab initio* and semiempirical methods including DFT have yielded insights going far beyond the purely empirical results of the application of e.g. the Hammett equation. These results in turn have suggested the application of thermodynamical concepts on results of spectroelectrochemical studies.

In attempts to widen the range of available process parameters and applicable monomers concepts of supramolecular host-guest chemistry have been applied by e.g. encapsulating monomers in cyclodextrines.

Following results of recent experimental studies and theoretical calculations illuminating the various aspects touched upon in the preceding introductory overview will be reviewed briefly.

### **Experimental**

For cyclic voltammetry (CV) gold (99.99%, Schiefer, Hamburg) embedded in epoxy ARALDIT D/HY 956 (Ciba special chemicals, Wehr/Baden, Germany) or platinum (99.99%, Schiefer, Hamburg) working electrodes embedded in glass were used. A gold or platinum sheet served as counter electrode, respectively. An Ag/AgCl electrode filled with the respective supporting electrolyte solutions was used as reference in studies employing electrolyte solutions based on organic solvents. In the case of aqueous electrolyte solutions relative hydrogen electrodes filled with the supporting electrolyte solutions according to Will <sup>[8]</sup> or a saturated calomel electrode were used.

UV-Vis spectra were recorded for homo- and copolymer films deposited on an optically transparent ITO-glass electrode (MERCK) in the supporting electrolyte solution in a standard 10 mm cuvette using a Shimadzu UV 2101-PC instrument (resolution 0.1 nm); a cuvette with the same solution and an uncoated ITO glass was placed in the reference beam. Composition of electrolyte solutions is given in the figure captions.

Substituted thiophenes were prepared and purified as described elsewhere<sup>[9, 10]</sup>, the purification of pyrroles (unsubstituted and substituted ones) as well as their encapsulation in 2,6-dimethyl- $\beta$ -cyclodextrin (CD) have been reported in the respective publications<sup>[11 - 13]</sup>.

Density functional theory (DFT)<sup>[14-17]</sup> of the three-parameter compound functional of Becke (B3LYP) was used to optimize the geometry as well as to calculate the ionization potentials of neutral thiophene compounds and total atomic spin densities of the radical cations. The 6-31G(d)<sup>[18-29]</sup> basis set was used to optimize the structures as well as the total spin densities, while the 3-21G(d)<sup>[30-36]</sup> basis set was used to calculate the ionization potentials for neutral and radical cations of the compounds. The geometric structures of neutral molecules were optimized under no constraints. Nearly planar structures were used as the initial states<sup>[37]</sup> because most of the crystalline oligothiophenes show planar conformations<sup>[38 - 40]</sup>. Ionization potentials were computed as the energy differences between the neutral molecule and the respective radical cation, in which the radical cation has the same molecular geometry as the neutral molecule (the Frank-Condon state was assumed for the cations). On the other hand, the geometric structures of the radical cations were optimized independently from the neutral molecules prior to the calculations of spin densities. Radical cations were treated as open shell systems (UB3LYP). All calculations were performed using the Gaussian-98W software<sup>[41]</sup>.

## Results and Discussion

### *Redox thermodynamics of thiophene-furan copolymers*

Oxidation and subsequent reduction<sup>§</sup> of ICPs may be considered basically as redox processes with species being present in their respective oxidized and non-oxidized (in this context of redox electrochemistry also: reduced) form. According to the Nernst equation for any given concentration a formal potential can be calculated according to

$$E = E_0 + \frac{R \cdot T}{n \cdot F} \ln \frac{c_{\text{ox}}}{c_{\text{red}}} = E_0 + \frac{R \cdot T}{n \cdot F} \ln \frac{[O]}{[R]} \quad (1)$$

---

<sup>§</sup> Frequently the neutral state is called the reduced state, this is obviously wrong, in particular when considering those polymers which can be reduced (i.e. *n*-doped) indeed in addition of being oxidized (i.e. *p*-doped).

with  $c_{\text{ox}}$  and  $c_{\text{red}}$  being the respective concentrations\*\* of the redox species. It has been proposed to derive these concentrations from UV-Vis spectra of polymer films<sup>[42]</sup>. A broad absorption band (A) appearing with the polythiophene PTh (see figure 2) in its neutral (non-oxidized) state around  $\lambda = 450$  nm (A) corresponds to the  $\pi \rightarrow \pi^*$ -transition in the thiophene units. Its width observed in our investigation in particular in the oxidized state (in the original report<sup>[42]</sup> no spectra are shown) implies the coexistence of segments with long as well as short effective conjugation lengths. The band width observed already in the neutral state which may not be attributed straightforwardly to the effect of conjugation may be due to residual oxidized segments present even in the reduced state, they may also be caused by intermolecular interactions in the polymer. Unfortunately this feature and further changes in the shape of the band as seen in Figure 2 may result in some uncertainty of the correlation between actual concentration of the studied species and the maximum absorption.

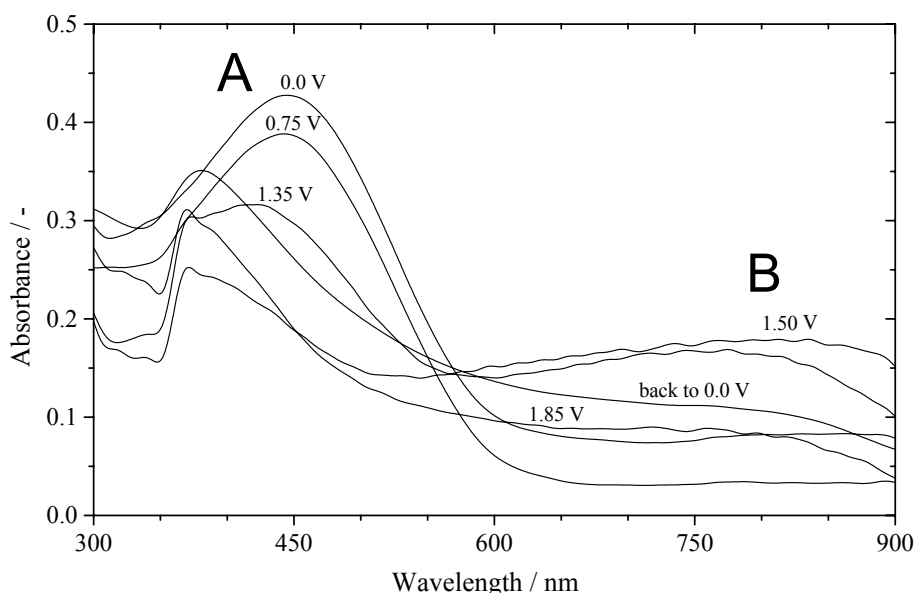


**Figure 2:** *In situ* UV-Vis spectra of an ITO-electrode coated with polythiophene prepared at  $E_{\text{Ag}/\text{AgCl}} = 1.65$  V in a BFEE + EE (ratio 1:2) solution containing 0.1 M thiophene and 0.1 M TBATFB recorded at different applied potentials in a solution of acetonitrile + 0.1 M TBATFB<sup>††</sup>.

\*\* In a more rigorous treatment activities have to be used instead, only at small concentrations activities can be replaced by concentrations. In the present discussion this detail is not considered, a suitable treatment of this problem has neither been developed nor described so far.

†† BFEE: Boron trifluoride-ethyl ether, EE: Ethyl ether, TBATFB: Tetrabutylammonium tetrafluoroborate

Upon oxidation, this absorption almost vanishes. Taking the absorbance at a selected wavelength (here: the absorption maximum of the neutral polymer form) as being related to the concentration according to the Lambert-Beer law the Nernst equation can be modified

$$E = E_0 + \frac{R \cdot T}{n \cdot F} \ln \frac{A_{\max} - A}{A - A_{\min}} \quad (2)$$

with  $A$  being the absorption at a given electrode potential applied to the polymer film and  $A_{\min}$  and  $A_{\max}$  being the minimum (fully oxidized state) and maximum (fully neutral (non-oxidized) state) absorptions. This approach may be valid when the system under investigation has only two redox states. The appearance of a quasi-isosbestic point in the UV-Vis spectra (figure 2) and of only one redox peak pair in the CVs as displayed in figure 3 associated with the redox process



supports this assumption. The peak shift of the low-wavelength peak as well as the extreme width of the high-wavelength peak suggest nevertheless, that both oxidized and reduced species show a considerable dispersion of the property responsible for the absorption maximum position.

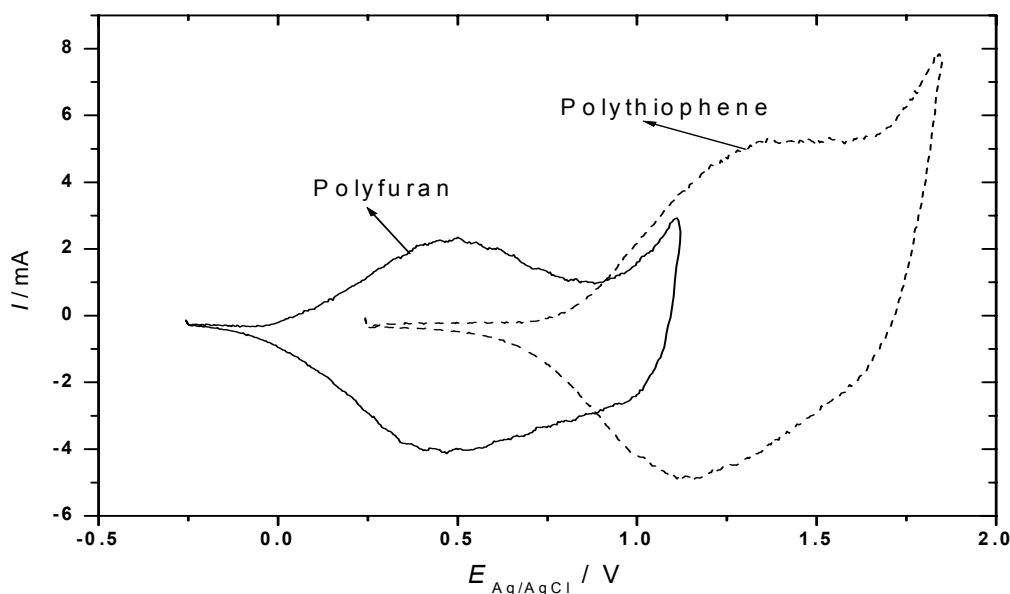


**Figure 3:** CVs of polymer films deposited on a platinum electrode recorded in a solution of acetonitrile + 0.1 M TBATFB,  $dE/dt = 100$  mV/s.

In the present case this is the energy difference between the participating electronic states, i.e. the respective HOMOs and LUMOs or – in case of band formation – the respective electronic bands in the polymer. As discussed elsewhere<sup>[43, 44]</sup> the width of the electronic absorption bands indicates a broad distribution of

conjugation lengths of the involved segments of the polymer chain. Accordingly the HOMOs involved in the electrooxidation process show a distribution of energy values. As previously discussed extensively in semiconductor electrochemistry redox systems in solution have been treated assuming similar distributions of states without making the use of the Nernst equation invalid <sup>[45]</sup>. Upon electrochemical oxidation a radical cation (elsewhere, in particular in solid state physics and chemistry, called polaron) is formed, it may extend over several monomer (repeat) units by conjugation (for a visualization see figure 4). The electrode potential where oxidation occurs may be taken as indicator of the HOMO energy, it cannot be compared directly with data taken from UV-Vis spectra. In the latter case excitation of an electron from the HOMO into a LUMO results in a bound exciton whereas in case of electrooxidation the final state is a charged species. Thus comparison of UV-Vis excitation energies with electrode potential differences may be misleading <sup>[46]</sup> ((electro)oxidation probes HOMOs, (electro)reduction probes LUMOs, the difference appears like a HOMO-LUMO difference at first glance). Even in cases where electrochemically the same site in a species is probed (this is not necessarily always the case) only careful correlations may be attempted. The band previously located around  $\lambda = 450$  nm decreases in intensity and shifts to higher energies (i.e. shorter wavelengths). This indicates a decreasing number of reduced species being available for optical excitation (thus in agreement with the Nernst equation approach outlined above), the band shift implies that these species are actually shorter conjugated segments of the polymer chain requiring higher excitation energy. The optical absorption (B) observed with the oxidized polymer around  $\lambda = 775$  nm is caused by a transition from the valence band into the upper polaron state <sup>[47]</sup>. With increasing degree of oxidation (and thus of doping and concentration of radical cations) these species (polarons in polaron states) combine pair-wise into spinless dication (bipolarons). The various states and energies depending on the degree of oxidation as well as allowed optical transitions (some of them already discussed above) are depicted in a band scheme in figure 5. As discussed above and in more detail elsewhere <sup>[46]</sup> the energy differences between bands and levels are not equivalent to the position of absorption maxima in UV-Vis spectra. In a simplified approach this is due to the fact, that optical excitation results initially in a bound exciton, a state and situation entirely different from the electrooxidation or – reduction products. Instead the onset of the respective absorption bands has been suggested to be taken in approximation as being equivalent to said energies. Obviously this does not remedy the fundamental problem and difference.

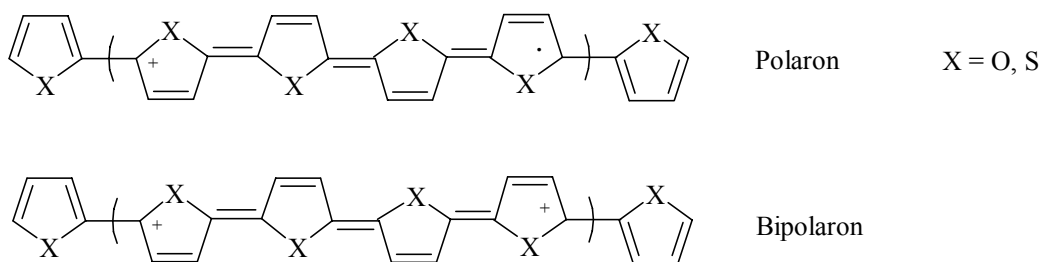


**Figure 4:** Conceivable polaron and bipolaron structures in polythiophene etc.

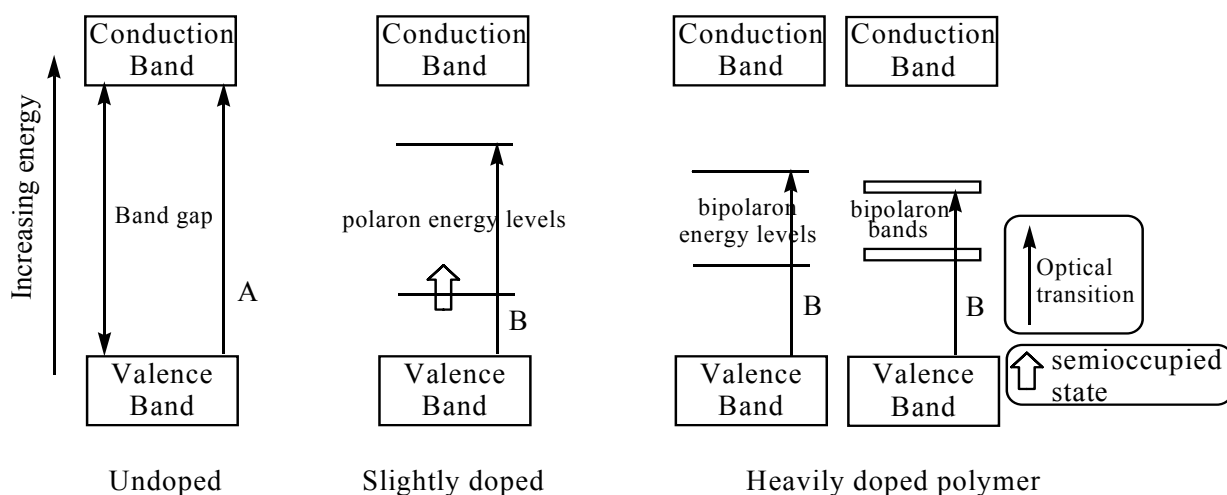
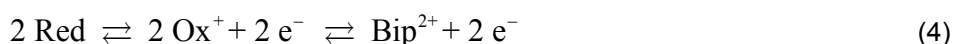


**Figure 5:** Energy levels, conduction and valence bands in polythiophene.

The simplified reaction scheme of the first transition has to be supplemented:



The latter step is a non-electrochemical one, thus it can be argued, that only the electrochemical first one has to be considered when setting up contributions towards the Nernst-equation. Contrary to ICPs where the polaron and bipolaron states could be separated easily by means of their distinctly different optical transitions this transition appears impossible with polythiophene or polyfuran. The extremely broad absorption extending only slightly into the NIR in case of polythiophene (see figure 2) may thus include absorptions from the valence band into the upper polaron and bipolaron state/band. This suggests using only the absorption A caused by the interband transition in setting up the Nernst equation. Spectral deconvolution based on the Alentsev-Fok method has been proposed to both identify and quantify various chemical species in polyaniline differing in state of oxidation, type of bonding etc. <sup>[48]</sup>. This approach might be helpful in treating complex UV-Vis spectra with the aim of elucidating concentrations of species involved in various redox equilibria. In case of polyaniline the existence of two redox peak pairs indeed suggests the presence of more than two electrochemically related redox states (as compared to only one in case

of polythiophene, polyfuran etc.). A further indicator of non-simple redox behavior (i.e. the presence of e.g. more than one redox equilibrium) is the absence of an isosbestic point as observed e.g. in case of polypyrrole. Despite the observation of only a single redox peak pair in the CV three distinct optical transitions (see below) can be observed.

Taking absorption data from the UV-Vis spectra displayed in figure 2 and from those of polyfuran and several furan-thiophene copolymers<sup>[49]</sup> Nernst-plots as shown in figure 6 were constructed. The value of  $E_0$  observed at  $[O]/[R] = 1$  is lower for polyfuran than for polythiophene as expected from the CVs (see figure 3). Further values corresponding to copolymers prepared at different feed ratios and different deposition electrode potentials  $E_{\text{pol}}$ , are collected in table 1<sup>[49]</sup>. With a growing fraction of furan in the feed the behavior of the copolymer as implied by the value of  $E_0$  approaches the behavior of polyfuran. A lower deposition potential favors incorporation of furan which is easier to electrooxidize<sup>[50]</sup> again resulting in a polyfuran-like behavior of the copolymer. The slope of the line in the Nernst-plot should be related to the number of electrons  $n$  transferred in the potential-determining step according to  $0.059/n$  [V]. The values of this slope as collected in table 1 are all in a range formally resulting in a value of approx.  $n = 0.25$ . This significantly “super-Nernstian”<sup>††</sup> behavior (sometimes also called “non-Nernstian behavior”<sup>[51]</sup>) has been observed repeatedly and discussed extensively before<sup>[42]</sup>. With reference to previous explanations of similar results<sup>[47]</sup> based on transferred charge and amount of polymer it has been suggested that this value implies a one-electron transfer from/to a four monomer unit segment of the polymer chain<sup>[49]</sup>, based on the arguments proposed so far this explanation remains speculative or at least rather unreliable because of the numerous assumptions fed into the stoichiometric calculations nevertheless (see also ref. [52]). Higher values of the slope correspond to higher values of  $E_0$ . A similar correlation found before [42] with differently substituted thiophenes has been attributed to the higher energy needed for polymer oxidation as expressed in higher values of  $E_0$  and correspondingly higher slopes.

**Table 1:** Thermodynamic data of selected ICPs

Furan/Thiophene (mole ratio)	$E_{\text{pol}}^* = 1.50$ V		$E_{\text{pol}} = 1.55$ V		$E_{\text{pol}} = 1.60$ V		$E_{\text{pol}} = 1.70$ V		Polyfuran $E_{\text{pol}} = 1.45$ V		Polythiophene $E_{\text{pol}} = 1.65$ V	
	$E_0$ /V	slope mV/log unit	$E_0$ /V	slope mV/log unit	$E_0$ /V	slope mV/log unit	$E_0$ /V	slope mV/log unit	$E_0$ /V	slope mV/log unit	$E_0$ /V	slope mV/log unit
1:1	0.96	252	0.98	260	1.20	262	1.22	274	0.42	216	1.27	262
4:1	0.71	237	0.79	248	0.87	254	0.94	268				
8:1	0.44	203	0.61	219	0.74	224	0.85	234				

\* $E_{\text{pol}}$ : electropolymerization potential

†† The term „hyper-Nernstian“ slope has been proposed elsewhere in symmetry with „hypo-Nernstian“ slope designating values smaller than 59 mV per decade.

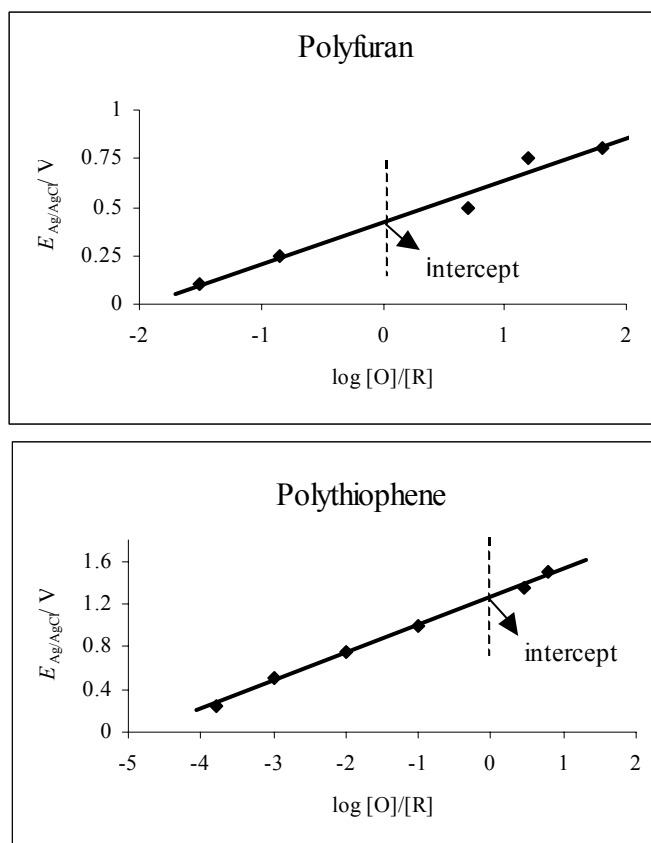


**Figure 6:** Nernst plots corresponding to the redox process of (a) polyfuran, (b) polythiophene.

Because the concentration of oxidized and reduced species is derived from optical data the value approx.  $n = 0.25$  may indeed suggest a conjugation length of four units based on the following line of arguments. Formal transfer of one electron results in a fourfold increase in the number of optically absorbing species. Assuming validity of Lambert-Beers law the observed optical absorption is proportional to the number of absorbing species, i.e. in the present case of systems showing a  $\pi \rightarrow \pi^*$ -transition. A fourfold increase (or decrease) of numbers of species showing this particular transition is possible only when transfer of one electron affects four repeat units in the polymer simultaneously, i.e. the transferred electron is (or was) delocalized along four units. This indeed is possible only when assuming a conjugation extending across four repeat units. Careful further examination of this explanation remains necessary because intrinsically polymers have apparently shown in many investigations broad distributions of length of conjugation.

#### *Theoretical studies of the mechanism of electropolymerization of substituted thiophenes*

Tools from theoretical chemistry can be combined with spectroelectrochemical data yielding insights going well beyond empirical correlations provided by e.g. the Hammett relationship<sup>[10, 53, 54]</sup>. In a study of the electrooxidation and –polymerization as well as subsequent doping/dedoping in both  $n$ - and  $p$ -doping regime we have applied

semiempirical calculation methods and DFT to predict trends in monomer and polymer properties. A selection of 3-(*p*-X-phenyl) thiophene monomers (X= -H, -CH<sub>3</sub>, -OCH<sub>3</sub>, -COCH<sub>3</sub>, -COOC<sub>2</sub>H<sub>5</sub>, -NO<sub>2</sub>) as depicted in figure 7 has been electrooxidized yielding polymer films which were subsequently *p*- and *n*-doped electrochemically<sup>[9, 10, 46, 37]</sup>. A correlation between oxidation potential and Hammett constant  $\sigma_p$  yields a less than satisfactory result (figure 8). With respect to *p*- and *n*-doping correlations were not substantially better, i.e. their predictive value remains limited. Taking into account that both inductive and resonance effects contribute to  $\sigma_p$  separate correlations were tried without substantial improvement. In addition, the fundamental limitation of the Hammett-concept remains: it is limited to aromatic compounds having substituents. As a first step away from this inherent limitation we have calculated semiempirically heats of formation  $\Delta H_f$  of the radical cations obtained in the initial monomer electrooxidation step (as previously used in a large selection of heteroatom-containing ligands frequently employed in organometallic chemistry<sup>[53]</sup>). The correlation – now free from assumptions regarding identity etc. of the involved compound and availability of experimental data – showed an only slightly better correlation. Variations in assumptions regarding properties of, e.g., the molecular environment (solvent, see figure 9) resulted in no significant improvement. A significantly better correlation was obtained between the energies of the HOMOs of the thiophenes (displayed in figure 10 as ionization energies  $E_i$ , the ionization energies<sup>§§</sup>  $E_i$  were assumed to be equal to the HOMO energies based on Koopman's theorem (for a thorough discussion of this somewhat controversial subject see e.g.<sup>[56, 57]</sup>)) and the oxidation potentials.

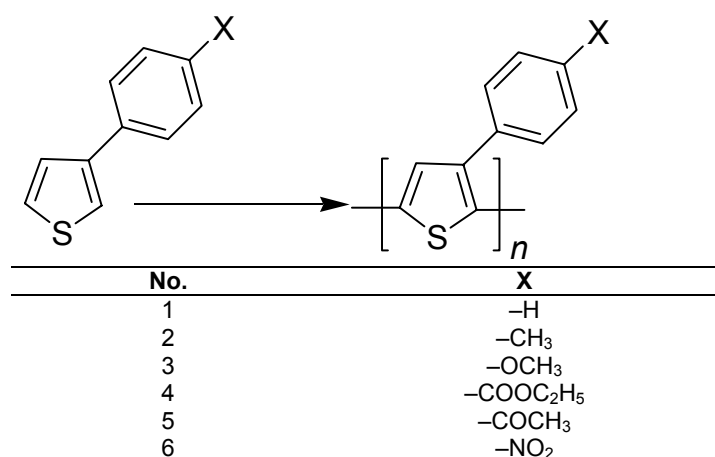


**Figure 7:** Investigated thiophenes.

<sup>§§</sup> The terminology is confusing. Ionization energies are frequently used to denote the energy needed to remove an electron from a single atom, whereas ionization potentials seem to be used for the respective process involving polynuclear species. In agreement with current recommendations of IUPAC [55] we use the suggested symbol  $E_i$ .

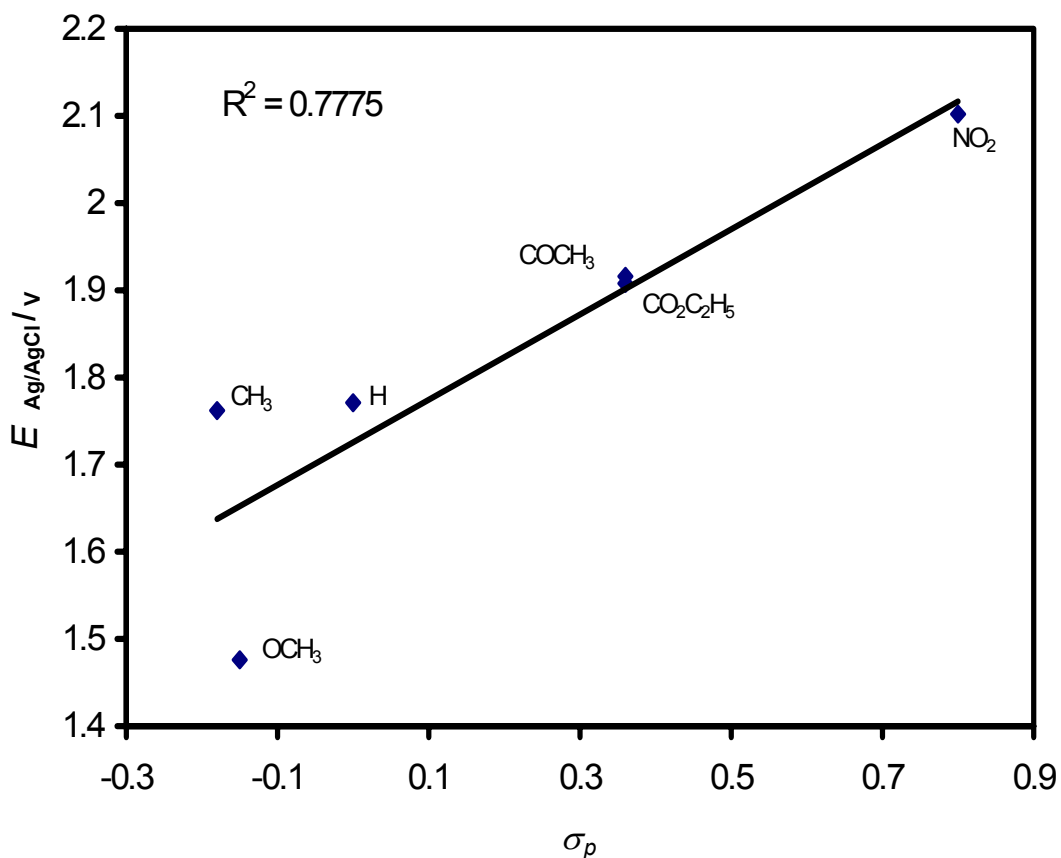


Figure 8: Plot of the oxidation potential of the monomers against  $\sigma_p$  values.

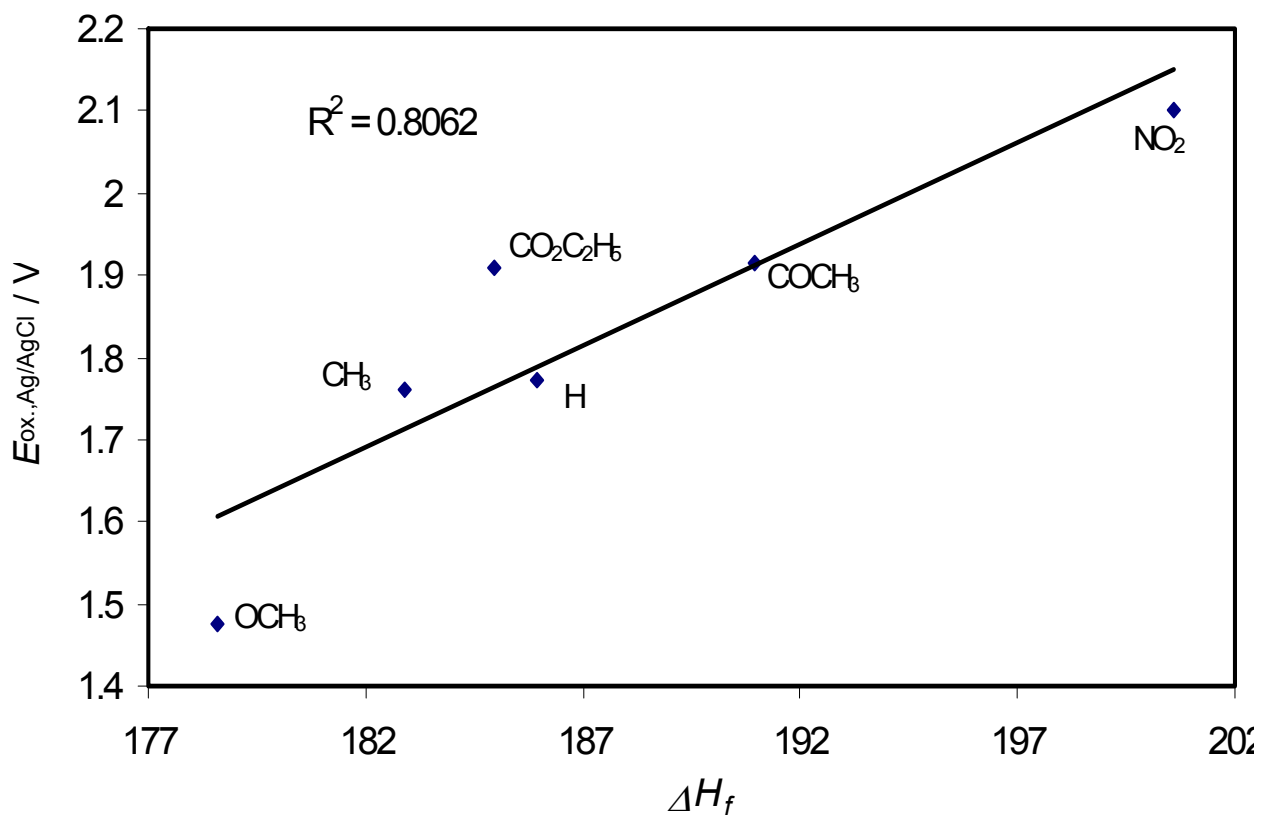
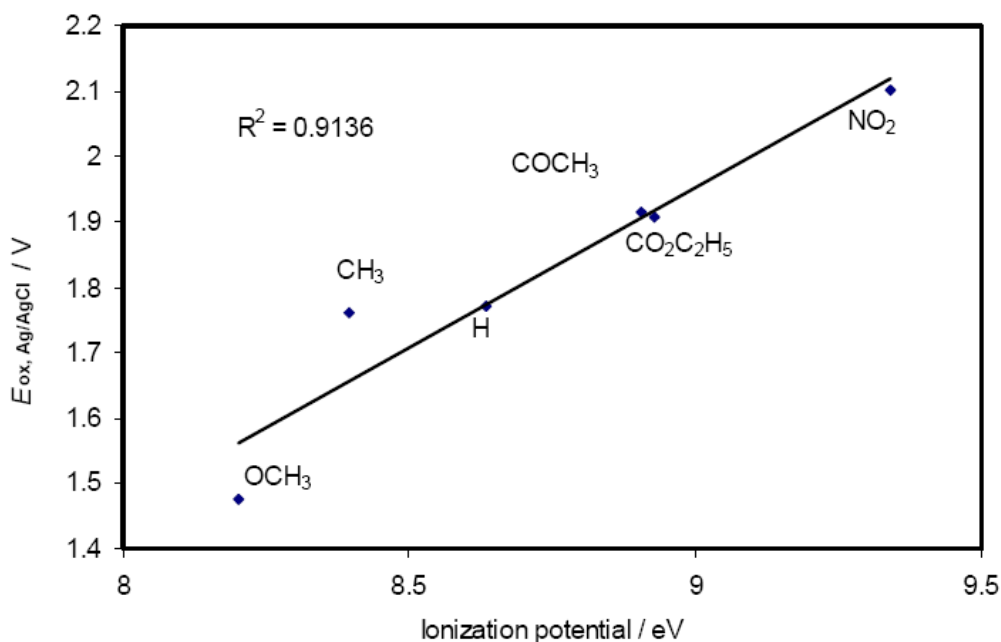


Figure 9: Plot of oxidation potentials of the monomers against heat of formation  $\Delta H_f$  in acetonitrile.



**Figure 10:** Plot of the oxidation potentials of the monomers against the HOMO energy.

#### *Polypyrroles prepared via host-guest chemistry*

Properties of ICPs as elucidated with electrochemical, spectroelectrochemical and numerous other methods obviously depend strongly on the experimental parameters set during their polymerization. A characteristic feature of ICPs prepared both via chemical and electrochemical routes is a rather broad distribution of chain lengths. In case of electropolymerization this seems to be related to the rate of radical cation formation. High rates, i.e. high anodic currents obtained by applying very positive electrode potentials, result in a large rate of oligomer nucleation and consequently a limited subsequent chain growth. Reduction of the rate of radical formation can be achieved obviously quite easily, this will result in a low rate of polymerization, in the worst case the polymerization will not start at all. Attempts to obtain more narrow chain length distributions include – besides the use of multiple phase systems (emulsions) <sup>[58]</sup> – the use of concepts of supramolecular chemistry. Molecules like pyrrole or thiophene can be loaded into the internal cavity of cyclodextrins (CD's) <sup>[59]</sup>. These are cyclic glucopyranose oligomers having a toroidal shape. The  $\alpha$ -,  $\beta$ - and  $\gamma$ -cyclodextrins contain six, seven or eight glucose units, respectively, and exhibit conical structures with a hydrophobic internal cavity and a hydrophilic exterior caused by the presence of hydroxyl groups. These compounds have the ability to form inclusion complexes with guest molecules of the proper size <sup>[60]</sup> as depicted schematically in figure 11. In case of monomer-loaded CDs this inclusion has several effects during the electropolymerization which is still possible: It may increase effective concentration of poorly water-soluble monomers in aqueous solution. In particular with these monomers this opens a route to electropolymerization

in aqueous solution instead of nonaqueous ones. Apparently it protects the radical cation formed with the monomer still inside the cavity by removal of an electron upon interaction between the inserted molecule and the electrode from nucleophilic attack of the solvent; otherwise the formation of polymers from aqueous solution impossible without CD or possible only with a dominant fraction of overoxidation just as a consequence of this attack would not be reasonable when performing the same electropolymerization with encapsulated monomers.

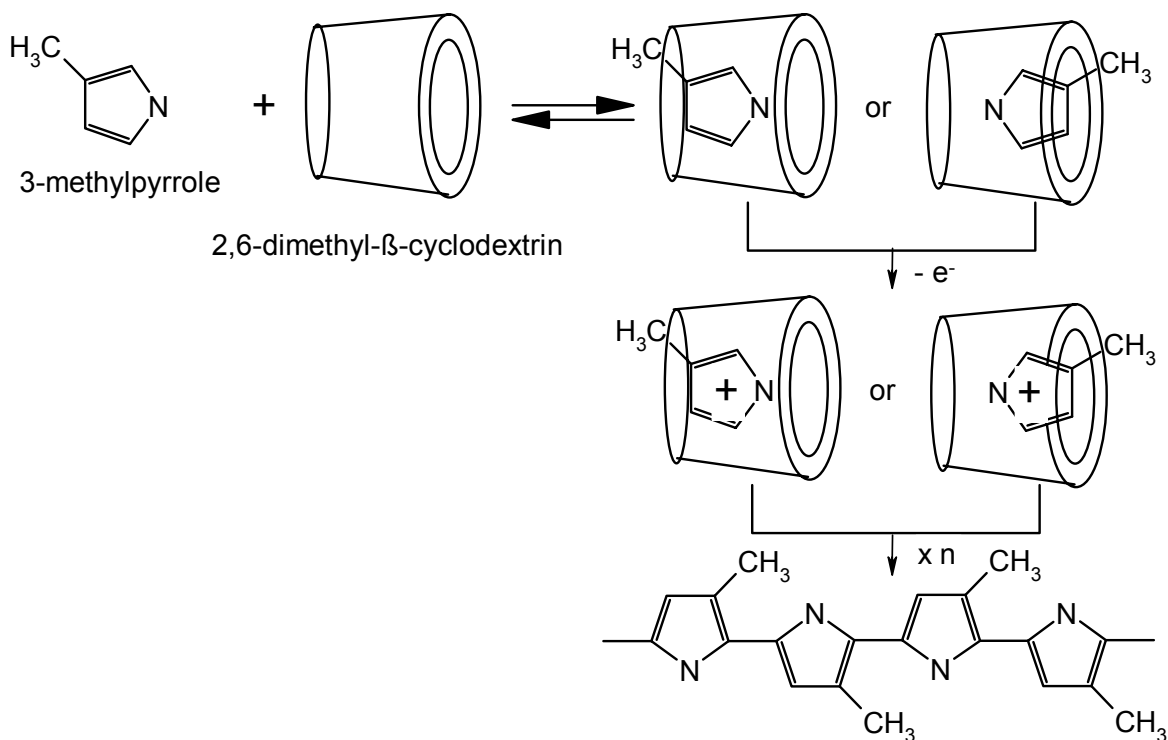


**Figure 11:** Schematic of the formation of CD-inclusion compounds

During electropolymerization by applying a cyclic electrode potential sequence (just as in CV) the oxidation peak associated with conversion of the pyrrole monomer into the radical cation a current peak is observed (see figure 12) which shifts towards more positive electrode potentials during subsequent cycling. The peak observed with the encapsulated monomer is observed at slightly more positive electrode potentials indicating some inhibition of the charge transfer. In nonaqueous solutions the current peak associated with monomer oxidation of 3MPy and (3MPy-β-DMCD) is less obvious (see figure 13) and hardly separated from the current associated with electrolyte solution decomposition. Again the oxidation is impeded somewhat with the encapsulated monomer as implied by the diminished current.

The redox behavior of the polymer films obtained with all studied monomers is significantly affected by the inclusion although no evidence of the presence of CD in the polymer has been found (neither as a constituent of a composite material nor as host of a polymer chain stringed within the CD). In reports by other authors only

circumstantial evidence of the presence of CD in various thiophene-related polymers has been reported <sup>[61]</sup>, no evidence of grafting of CD on the polymer chains of these polymers has been presented in this report or elsewhere <sup>[62, 63]</sup>. Results of studies with an electrochemical quartz microbalance obtained with bithiophene and hydroxypropyl- $\beta$ -cyclodextrine seem to indicate the presence of a small amount of CD in the polymer, but no convincing evidence of grafting was obtained, instead cyclodextrine insertion by chain encapsulation was suggested. Claims of CD-grafting presented recently <sup>[64]</sup> could not be substantiated.

CVs of polymers of 3MPy and (3MPy- $\beta$ -DMCD) during polymerisation as displayed in figure 14 demonstrate the formation of redox active polymer films with the encapsulated monomer showing only a slightly lower rate of growth. The current peaks observed with poly-3MPy are narrow as compared to those observed with poly(3MPy- $\beta$ -DMCD). Taking the electrode potential where a segment of the polymer chain is oxidized as a measure of the respective HOMO-energy a narrow peak implies a narrow distribution of HOMO-energies and thus of length of conjugated segments. Apparently based on these electrochemical data the distribution is broader with poly(3MPy- $\beta$ -DMCD). These differences are illustrated in figure 15 with polymer film-coated electrodes in supporting electrolyte solution only. This simplified approach towards understanding peak shapes and their changes in cyclic voltammograms assumes the presence of discrete species in solution with discrete HOMO-energies. The development of a peak in a CV depends instead on further complicating contributions, in particular diffusion of species and evolution of concentration gradients at the electrochemical interface. In case of ICPs the situation is even more complicated because of the presence of a more or less extended interphase at the electrochemical interface. The peak shapes frequently observed differ substantially from those observed with dissolved species, details have been discussed previously elsewhere <sup>[65, 66]</sup>. Accordingly the explanation of the change in peak shape observed here as being indicative of a changed distribution of length of conjugated segments is speculative at best.

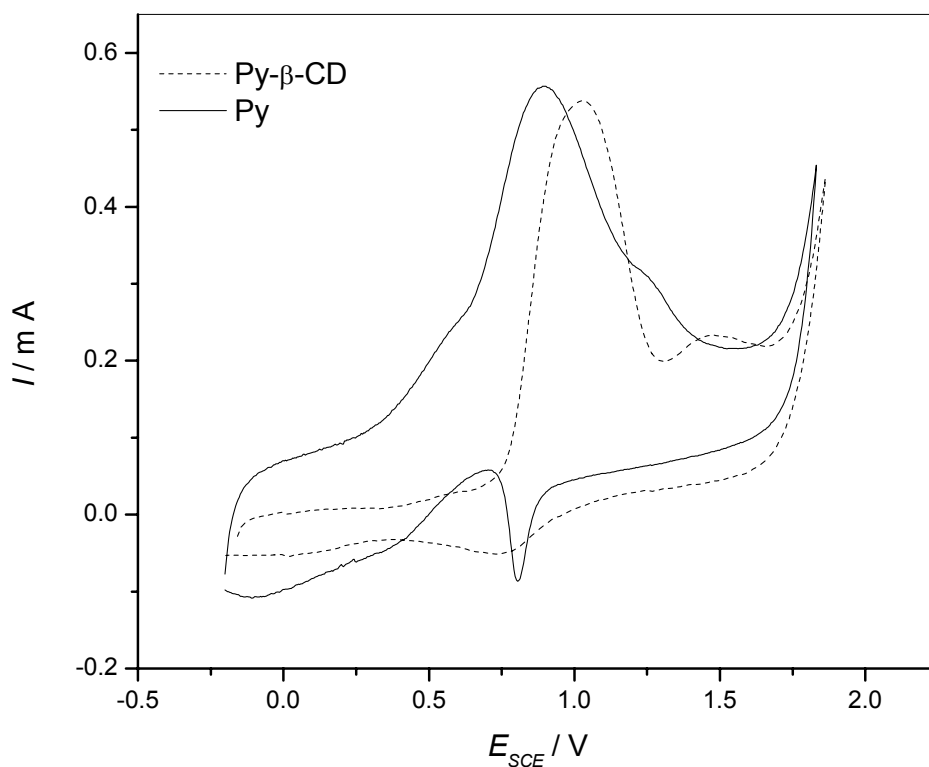


**Figure 12:** Cyclic voltammograms of a gold electrode in solutions of 0.1 M pyrrole (solid line) and 0.05 M pyrrole-cyclodextrin (dashed line) in an aqueous solution of 0.1 M LiClO<sub>4</sub>,  $dE/dt = 50\text{mV/s}^{-1}$ .

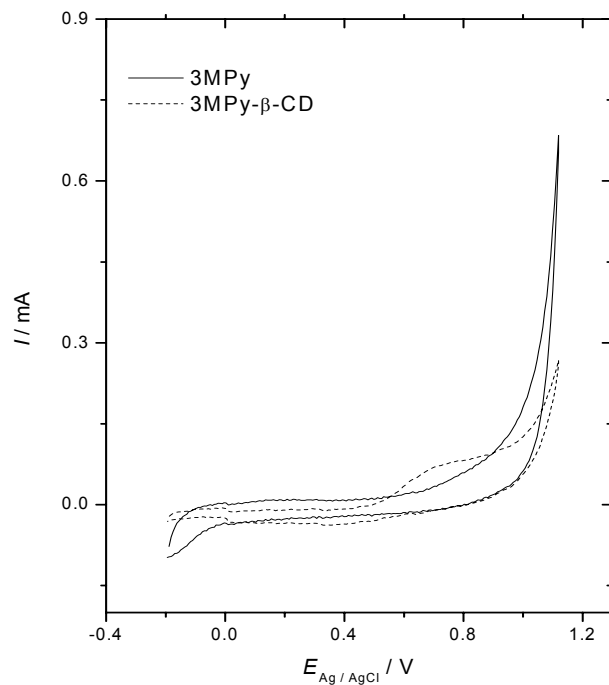


**Figure 13:** Cyclic voltammograms of a gold electrode in a solution of 3MPy<sup>\*\*\*</sup> (solid line) and (3MPy-β-DMCD) complex (dashed line) in acetonitrile + 0.05 M LiClO<sub>4</sub>,  $-0.20 < E_{\text{Ag}/\text{AgCl}} < 1.10\text{ V}$ ,  $dE/dt = 50\text{ mV}\cdot\text{s}^{-1}$ .

\*\*\* 3MPy: 3-methylpyrrole

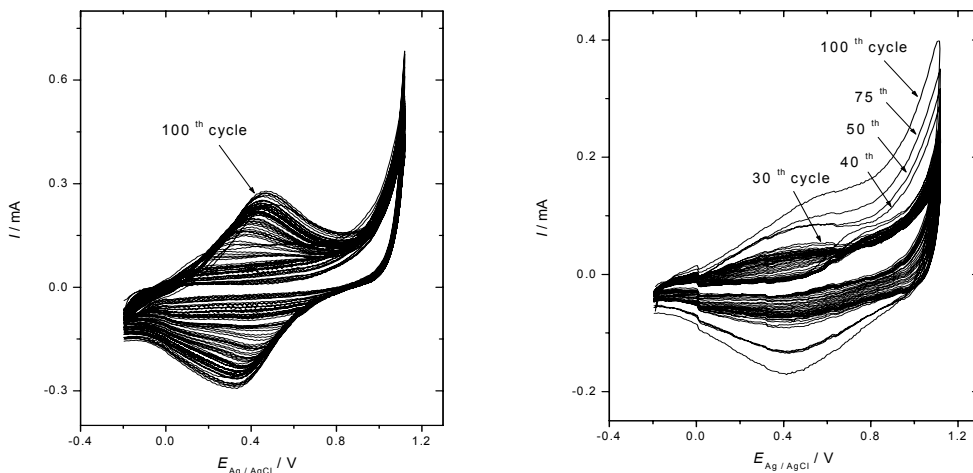


**Figure 14:**

**Left:** CVs (1,..., 100<sup>th</sup> cycle) during formation of P3MPy in a solution of 0.038 M 3MPy in acetonitrile + 0.05 M LiClO<sub>4</sub>,  $-0.20 < E_{\text{Ag}/\text{AgCl}} < 1.10$  V, gold electrode,  $dE/dt = 50$  mV·s<sup>-1</sup>.

**Right:** CVs (1,..., 30, 40, 50, 75, 100<sup>th</sup> cycle) during formation of poly(3MPy-β-DMCD) complex in a solution of 0.038 M (3MPy-β-DMCD) complex in acetonitrile + 0.05 M LiClO<sub>4</sub>,  $-0.20 < E_{\text{Ag}/\text{AgCl}} < 1.10$  V at a gold electrode,  $dE/dt = 50$  mV·s<sup>-1</sup>.

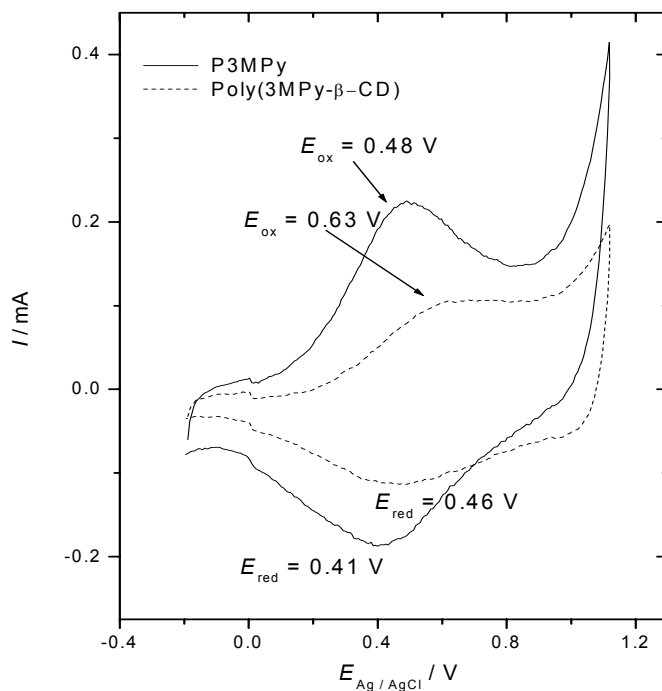


**Figure 15:** CVs of a gold electrode coated with P3MPy (solid line) and poly(3MPy-β-DMCD), (dashed line) in a blank solution of acetonitrile + 0.05 M LiClO<sub>4</sub>,  $dE/dt = 50$  mV·s<sup>-1</sup>.

More reliable information may be gleaned from UV-Vis spectroscopy. A comparison of spectra obtained both with poly-3MPy and poly(3MPy- $\beta$ -DMCD) (figure 16) shows three absorption features. A is assigned to the  $\pi \rightarrow \pi^*$ -transition. B is due to the high-energy polaronic transition <sup>[67]</sup> (as displayed in the schematic (figure 17) this transition refers to excitation from the valence band into the anti-binding (upper) polaron state <sup>[68]</sup>). C (not to be confused with C') as observed with significant intensity only at higher degrees of oxidation/doping is caused by a transition from the valence band into the lower bipolaron band, a more detailed discussion has been provided elsewhere <sup>[13]</sup>. With poly-3MPy the absorption peak is well within the visible region of the spectrum indicating a much shorter length of conjugation as for poly(3MPy- $\beta$ -DMCD) with the maximum in the NIR-region. The considerable blue-shift of the former absorption with increasing electrode potential indicates formation of radical cations with successively shorter conjugation length at higher electrode potentials indicating a significantly broader distribution of chain lengths. With poly(3MPy- $\beta$ -DMCD) the very weak absorption C shows a small shift only, the absorption shoulder observed at the long-wavelength edge of the spectrum seems to indicate such a shift also. Because the absorption maximum in the latter case is located in the NIR a verification was not possible in this study. Apparently the major absorption related to the presence of bipolarons is in the NIR-range indicating longer conjugated polymer segments formed with the encapsulated monomer. At first glance it is tempting to correlate this with the electronic conductance. The macroscopically measured conductance is a convoluted property depending on the concentration of mobile charge carrier (which may be measurable with UV-Vis spectroscopy in case all charge carriers show a well defined absorption band caused exclusively by their presence) and the mobility of these charge carriers (along the molecular chain, this step may indeed be related with conjugation length with a greater length improving undisturbed mobility, and between molecular strands in fibrils and between fibrils, for a detailed discussion see references [6,69]). Thus it might be assumed that poly(3MPy- $\beta$ -DMCD) shows a higher conductance. Actually the conductance is slightly lower in the doped state <sup>[13]</sup>. This does not necessarily contradict the line of argument given above, because the obtained data are not specific ones (conductivity) and because the length of conjugation is just one factor.

It seems noteworthy at this point to address two different features in both CVs and UV-Vis spectra related to the distribution of conjugation lengths. A broad UV-Vis absorption band is indicative of a spread of energies of the involved lower as well as upper states with a more narrow distribution of energies in either one or both states resulting in a sharper absorption band <sup>[44]</sup>. A shift of the band maximum (irrespective of the band shape, its width) as a function of applied electrode potential (i.e. state of oxidation/doping) implies a more or less extended variation of HOMO-energies, from the HOMOs electrons are removed upon electrooxidation. Thus a shift (practically

always for obvious reasons a blue-shift) detected with UV-Vis spectroscopy is indicative of a distribution of length of conjugation more reliably than the width of the current peak in the CV.

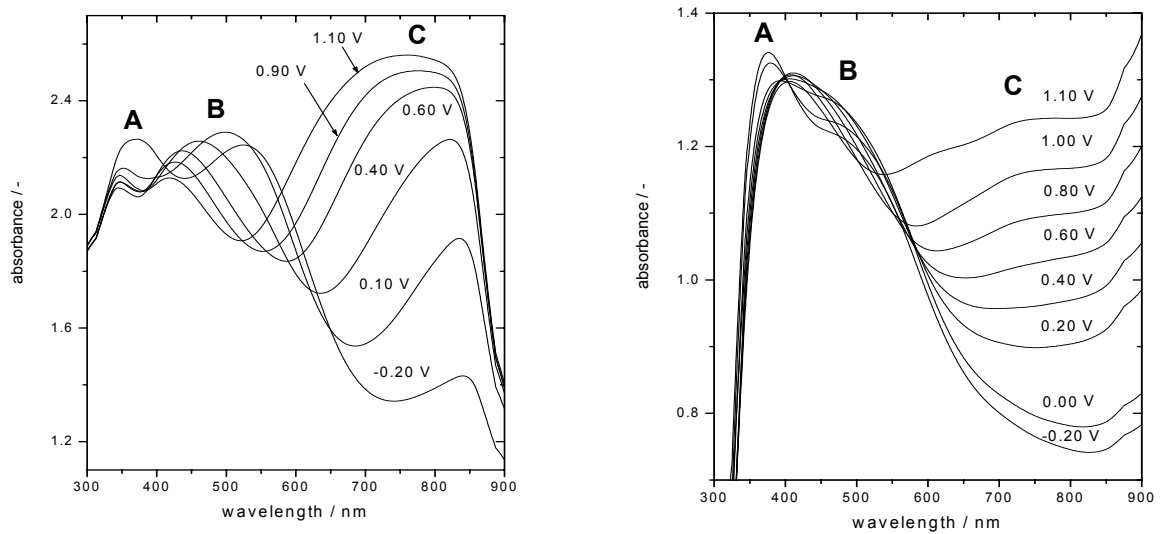


**Figure 16:**

**Left:** UV-Vis-spectra for P3MPy deposited potentiodynamically by cycling the potentials from  $-0.20 < E_{\text{Ag}/\text{AgCl}} < 1.10$  V in solution of  $0.038 \text{ M}$  3MPy in acetonitrile +  $0.05 \text{ M}$   $\text{LiClO}_4$  at different oxidation stages.

**Right:** UV-Vis-spectra for poly(3MPy-β-DMCD) deposited potentiodynamically by cycling the potentials from  $-0.20 < E_{\text{Ag}/\text{AgCl}} < 1.10$  V in solution of  $0.038 \text{ M}$  poly(3MPy-β-DMCD) in acetonitrile +  $0.05 \text{ M}$   $\text{LiClO}_4$  at different oxidation stages.

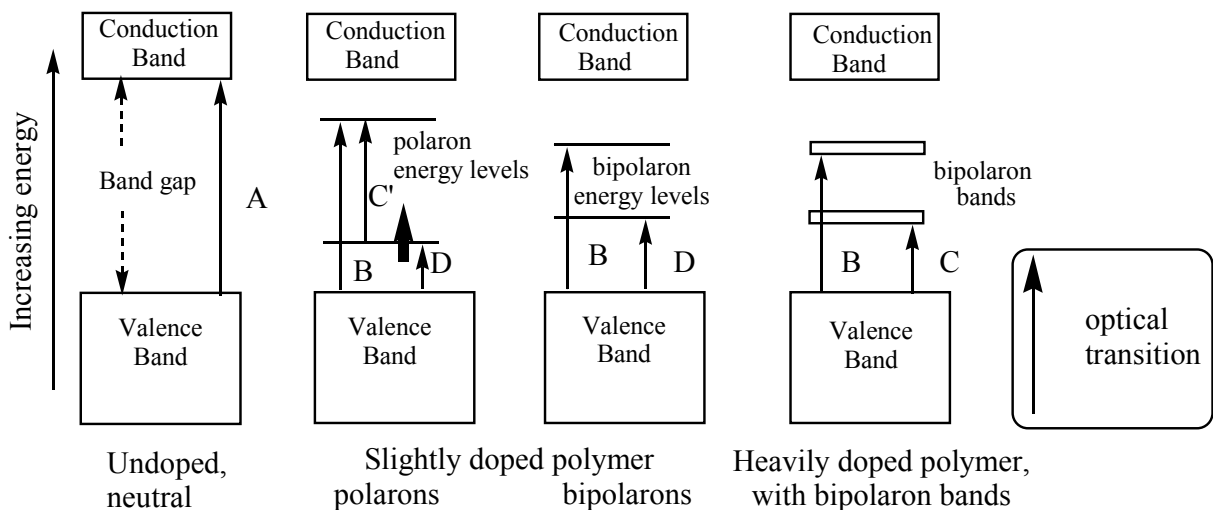


**Figure 17:** Electronic band diagrams for P3MPy and poly(3MPY-β-DMCD) films. A = band gap transition ( $\pi \rightarrow \pi^*$ ); B, C, D = electronic transitions; bold arrow = unpaired electron, semi-occupied level.

With poly-N-methylpyrrole (PNMPy) and poly(NMPy- $\beta$ -DMCD) verification is more straightforward. UV-Vis spectra displayed in figure 18 show again three transitions which can be assigned in exactly the same way as above. The long wavelength transition observed with PNMPy is at the edge of the spectrum implying a rather large length of conjugation. Upon oxidation the onset of this band and thus presumably the band itself seems to blue-shift somewhat indicating said distribution of chain length. With poly(NMPy- $\beta$ -DMCD) peak position and width remain almost completely unchanged upon oxidation (doping) indicating a very small dispersion of HOMO-energies and thus length of conjugation.

Encapsulation of pyrrole monomers has – although CD is not present in the polymers according to our knowledge – a significant influence on the polymer. As discussed elsewhere<sup>[12,13]</sup> this can be rationalized taking into account the electropolymerization mechanism. As already implied by the slightly higher oxidation potentials of the encapsulated monomers and the associated anodic currents being somewhat lower the monomers have to be released from the CD, this process appears to be slow. It limits consequently the local concentration of free radicals in front of the electrode available for chain initiation and continuation (and also for detrimental nucleophilic attack by other solution constituents) resulting in a more “orderly” chain growth and thus a more narrow distribution of chain length. The actual average chain length may differ substantially between various polymers as demonstrated above.

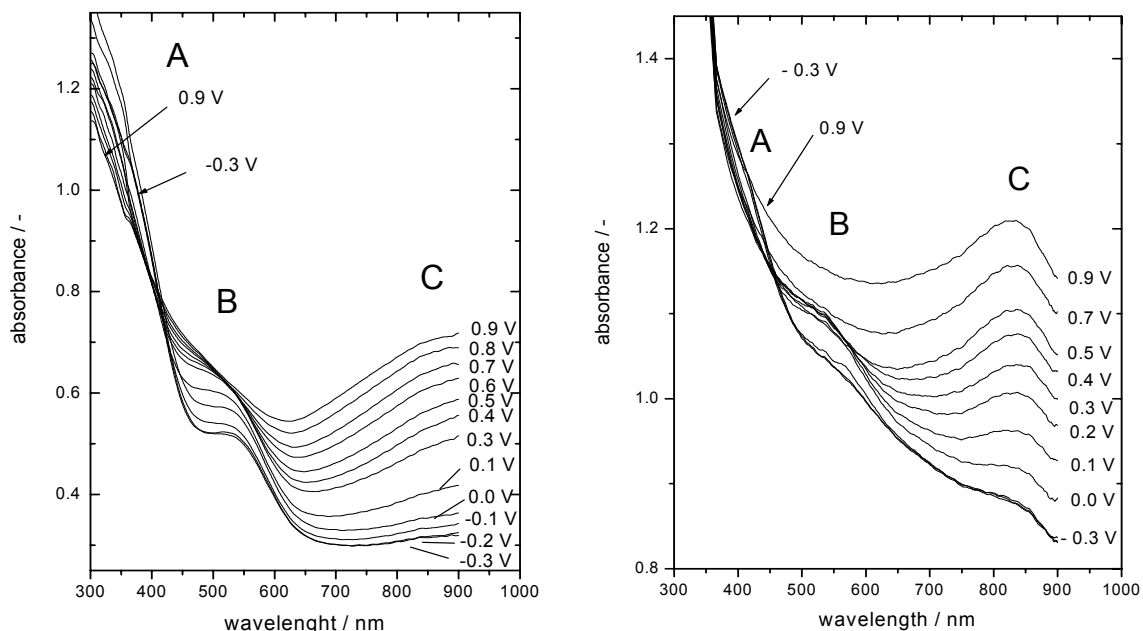


**Figure 18:**

**Left:** UV-Vis-spectra of an ITO-electrode coated with PNMPy in a solution of acetonitrile + 0.1 M LiClO<sub>4</sub> deposited potentiodynamically with  $-0.20 < E_{Ag/AgCl} < 0.90$  V in a solution of acetonitrile + 0.1 M LiClO<sub>4</sub> at different electrode potentials.

**Right:** UV-Vis-spectra for poly(NMPy- $\beta$ -DMCD) films in a solution of acetonitrile + 0.1 M LiClO<sub>4</sub> deposited potentiodynamically with  $-0.20 < E_{Ag/AgCl} < 0.90$  V in a solution of acetonitrile + 0.1 M LiClO<sub>4</sub> at different electrode potentials.

## Conclusions

Using suitable combinations of complementary electrochemical, spectroscopic and theoretical methods deeper insights into structure-property relationships of intrinsically conducting polymers can be identified. They are corroborated by results of theoretical treatments which – despite their apparent limitations – may provide venues to more rational planning of synthetic experiments and tailored polymers.

In case of furan-thiophene copolymers optical data were used to elucidate redox thermodynamics of the homo- and copolymers. The observed trends in formal potentials fit well with results obtained from non-stationary studies of these polymers.

Electropolymerization of unsubstituted and substituted thiophenes proceeds via radicals. Using DFT radical intermediates, in particular their internal spin density distribution, can be studied. Polymer structures proposed on the basis of these calculations match very well experimentally observed ones supporting the suggested reaction mechanism.

Using cyclodextrins as host for both unsubstituted and substituted pyrrole intrinsically conducting polymers can be obtained both from aqueous and nonaqueous electrolyte solutions. The involvement of the host – which is apparently absent from the polymeric product – results in changes of the distribution of conjugation length (i.e. the optical properties) of the polymer which can be straightforwardly understood based on an encapsulation equilibrium between host and guest preceding the electrooxidation of the monomer.

## Acknowledgments

Financial support from the Fonds der Chemischen Industrie, the Deutsche Forschungsgemeinschaft (Graduiertenkolleg GRK 829/1) and the Deutscher Akademischer Austauschdienst DAAD is gratefully acknowledged. We are grateful to K. Banert for helpful discussions and support in synthesis of the thiophene monomers and to H.-J. Schäfer, S. Spange and A.A. Auer for stimulating discussions. New insights on UV-Vis spectroscopy and redox thermodynamics were provided by V.V. Malev and V.V. Kondratev, generous support of this exchange by the DAAD and St. Petersburg State University is appreciated.

## References

- [1] Holze, R.: Landolt-Börnstein: Numerical Data and Functional Relationships in Science and Technology, New Series, Group IV: Physical Chemistry, Volume 9A: Electrochemistry, Subvolume A: Electrochemical Thermodynamics and Kinetics, W. Martienssen, M.D. Lechner Eds, Springer-Verlag, Berlin 2007.
- [2] R. Holze: "Surface and Interface Analysis: An Electrochemists Toolbox", Springer Verlag, Heidelberg 2009.
- [3] Shirakawa, H.; Louis, E.J.; MacDiarmid, A.G.; Chiang, C.K.; Heeger, A.J., *Chem. Comm.* 1977, 578.
- [4] Shirakawa, H., *Synth. Met.* 2002, 125, 3.
- [5] Diaz, A.F.; Kanazawa, K.K., *J. Chem. Soc. Chem. Commun.* 1979, 635.
- [6] Holze, R. in: Handbook of Advanced Electronic and Photonic Materials and Devices, Vol. 8 (Nalwa, H.S.; Ed.), Academic Press, San Diego 2001, p. 209; Holze, R. in: "Advanced Functional Molecules and Polymers", Vol. 2 (Nalwa, H.S.; Ed.) Gordon&Breach, Amsterdam 2001, p. 171.

- [7] Brédas, J.L.; Andre, J.M.; Themans, B., *Phys. Rev. B - Cond. Mat.*, 1983, 27, 7827; Brédas, J.L.; Scott, J.C.; Street, G.B.; Yakushi, K.; *Phys. Rev. B - Cond. Mat.*, 1984, 30, 1023.
- [8] Will, F.G.; Hess, H.J., *J. Electrochem. Soc.*, 1986, 133, 454; Will, F.G.; Hess, H.J., *J. Electrochem. Soc.*, 1973, 120, 1.
- [9] Alhalasah, W.; Holze, R., *Microchim. Acta*, 2006, 156, 133.
- [10] Alhalasah, W.; R. Holze, *J. Solid State Electrochem.*, 2005, 9, 836.
- [11] Arjomandi, J.; Holze, R., *J. Solid State Electrochem.* 2007, 11, 1093.
- [12] Arjomandi, J.; Holze, R., *Synth. Met.*, 2007, 157, 1021.
- [13] Arjomandi, J.; Holze, R., *Cent. Eur. J. Chem.*, 2008, 6, 199
- [14] Hohenberg, P.; Kohn, W., *Phys. Rev.*, 1964, 136, B864.
- [15] Kohn, W.; Sham, L.J., *Phys. Rev.*, 1965, 140, A1133.
- [16] "The Challenge of d and f Electrons", Salahub, D.R.; Zerner, M. C.; Eds., American Chemical Society, Washington, D.C., 1989.
- [17] Parr, R.G.; Yang, W., "Density-functional theory of atoms and molecules", Oxford University Press, Oxford, 1989.
- [18] Ditchfield, R.; Hehre, W.J.; Pople, J.A., *J. Chem. Phys.*, 1971, 54, 724.
- [19] Hehre, W.J.; Ditchfield, R.; Pople, J.A., *J. Chem. Phys.*, 1972, 56, 2257.
- [20] Hariharan, P.C.; Pople, J. A., *Mol. Phys.*, 1974, 27, 209.
- [21] Gordon, M.S., *Chem. Phys. Lett.*, 76 (1980) 163.
- [22] Hariharan, P.C.; Pople, J. A., *Theo. Chim. Acta*, 1973, 28, 213.
- [23] Blaudeau J.-P., McGrath, M. P.; Curtiss, L.A.; Radom, L., *J. Chem. Phys.*, 1997, 107, 5016.
- [24] Francl, M.M.; Pietro, W.J.; Hehre, W.J.; Binkley, J.S., DeFrees, D.J.; Pople, J.A.; Gordon, M.S., *J. Chem. Phys.* 1982, 77, 3654.
- [25] Binning Jr, R.C.; Curtiss, L.A., *J. Comp. Chem.* 1990, 11, 1206.
- [26] Rassolov, V.A.; Pople, J.A.; Ratner, M.A.; Windus, T L., *J. Chem. Phys.*, 1998, 109, 1223.
- [27] Rassolov, V.A.; Ratner, M.A.; Pople, J.A.; Redfern, P.C.; Curtiss, L.A., *J. Comp. Chem.*, 2001, 22, 976.
- [28] Petersson, G.A.; Al-Laham, M.A., *J. Chem. Phys.*, 1991, 94, 6081.
- [29] Petersson, G.A.; Bennett A.; Tensfeldt, T.G.; Al-Laham, M.A.; Shirley, W.A.; Mantzaris, J., *J. Chem. Phys.*, 1988, 89, 2193.
- [30] Binkley, J.S.; Pople, J.A.; Hehre, W.J., *J. Amer. Chem. Soc.*, 1980, 102, 939.
- [31] Gordon, M.S.; Binkley, J.S.; Pople, J.A.; Pietro, W.J.; Hehre, W.J.; Amer, J., *Chem. Soc.*, 1982, 104, 2797.
- [32] Pietro, W.J.; Francl, M.M.; Hehre W.J.; Defrees, D.J.; Pople, J.A.; Binkley, J.S., *J. Am. Chem. Soc.*, 1982, 104, 5039.
- [33] Dobbs, K.D.; Hehre, W.J., *J. Comp. Chem.*, 1986, 7, 359.
- [34] Dobbs, K.D.; Hehre, W.J., *J. Comp. Chem.*, 1987, 8, 861.
- [35] Dobbs, K.D.; Hehre, W.J., *J. Comp. Chem.*, 1987, 8, 880.
- [36] Clark, T.; Chandrasekhar, J.; Spitznagel, G.W.; Schleyer, P.v.R., *J. Comp. Chem.*, 1983, 4, 294.
- [37] For further details see: Alhalasah, W.; Holze, R., *Electrochemical Society Transactions*, 2007, 2(3), 45.
- [38] Pelletier, M.; Brisse, F., *Acta Crystallogr., Section C. Cryst. Struct. Commun.*, 1994, 50, 1942.
- [39] Paulus, E.F.; Dammel, R.; Kampf, G.; Wegener, P.; Siam, K.; Wolinski, K.; Schafer, L., *Acta Crystallogr., Section B, Struct. Sci.*, 1988, 44, 509.
- [40] Barbarella, G.; Zambianchi, M.; Bongini A.; Antolini, L., *Adv. Mater.*, 1992, 4, 282.
- [41] Gaussian 98, Revision A.3, Frisch, M.J.; Trucks, G.W.; Schlegel, H.B., Scuseria, G.E., Robb, M.; Cheeseman, J.R., Zakrzewski, V.G., Montgomery, J.A.; Jr.; Stratmann, R.E.; Burant, J.C.; Dapprich, S.; Millam, J.M.; Daniels, A.D.; Kudin, K.N.; Strain, M.C.; Farkas, O.; Tomasi, J.; Barone, V.; Cossi, M.; Cammi, R.; Mennucci, B.; Pomelli, C.; Adamo, C.; Clifford, S.; Ochterski, J., Petersson, G. A., Ayala, P.Y.; Cui, Q.; Morokuma, K.; Malick, D. K.; Rabuck, A. D.; Raghavachari, K.; Foresman, J. B.; Cioslowski, J.; Ortiz, J. V.; Stefanov, B. B.; Liu, G.; Liashenko, A.; Piskorz, P.; Komaromi, I.; Gomperts, R.; Martin, R. L.; Fox, D. J.; Keith, T.; Al-Laham, M.A.; Peng, C. Y.; Nanayakkara, A.; Gonzalez, C.; Challacombe, M.; Gill, P.M.W.; Johnson, B.; Chen, W.; Wong, M.W.; Andres, J.L.; Gonzalez, C., Head-Gordon, M.; Replogle, E.S.; Pople, J.A., Gaussian, Inc., Pittsburgh, 1998.
- [42] Marque, P.; Roncali, J., *J. Phys. Chem.*, 1990, 94, 8614.
- [43] Alakhras, F.; Holze, R., *Synth. Met.*, 2007, 157, 109.
- [44] Brandl, V.; Holze, R., *Ber. Bunsenges. Phys. Chem.*, 1997, 101, 251.
- [45] Gerischer, H., *Electrochim. Acta*, 1990, 35, 1677.

- [46] Alhalasah, W.; Holze, R., *J. Solid State Electrochem.*, 2007, 11, 1605.
- [47] Glenis, S.; Benz, M.; LeGoff, E.; Schindler, J.L.; Kannewurf, C.R.; Kanatzidis, M.G., *J. Am. Chem. Soc.*, 1993, 115, 12519.
- [48] Nekrasov, A.A.; Ivanov, V.F.; Vannikov, A.V., *Russ. J. Electrochem.* 2000, 36, 883-1001.
- [49] Alakhras, F.; Holze, R., *Electrochim. Acta*, 2007, 52, 5896.
- [50] Alakhras, F.; Holze, R., *J. Appl. Polym. Sci.*, 2008, 107, 1133.
- [51] Diaz, A.F.; Castillo, J.I.; Logan, J.A.; Lee, W.-Y., *J. Electroanal. Chem.*, 1981, 129, 115.
- [52] Feldberg, S.W., *J. Am. Chem. Soc.*, 1984, 106, 4671.
- [53] Vatsadze, S.; Al-Anber, M.; Holze, R.; Thiel, W.R.; Lang, H., *Dalton Trans.*, 2005, 3632; Vatsadze, S.; Al-Anber M., Thiel, W.R.; Lang, H.; Holze, R., *J. Solid State Electrochem.*, 2005, 9, 764.
- [54] Zuman, P.: "Substituent Effects in Organic Polarography", Plenum Press, New York, 1967.
- [55] Größen, "Einheiten und Symbole in der Physikalischen Chemie" (IUPAC Ed.), VCH, Weinheim 1996.
- [56] Chong, D.P.; Gritsenko, O.V.; Baerends, E.J., *J. Chem. Phys.*, 2002, 116, 1760.
- [57] Bickelhaupt, F.M.; Baerends, E.J. in: Reviews in Computational Chemistry Vol. 15 (Lipkowitz, K. B.; Boyd, D. R., Eds.) Wiley-VCH, New York 2000, p. 1.
- [58] Shreepathi, S.; Holze, R., *Langmuir*, 2006, 22, 5196; Shreepathi, S.; Holze, R., *Chem. Mater.* 2005, 17, 4078; Shreepathi, S.; Van Hoang, H.; Holze, R., *J. Electrochem. Soc.*, 2007, 154, C67; Shreepathi, S.; Holze, R., *Macromol. Chem. Phys.*, 2007, 208, 609.
- [59] Storsberg, J.; Ritter, H.; Pielartzik, H.; Groenendaal, L., *Advan. Mater*, 2000, 12 567.
- [60] Chen, W.; Wan, X.; Xu, N.; Xue, G., *Macromolecules*, 2003, 36, 276.
- [61] Lagrost, C.; Lacroix, J.C.; Aeiyaich, S.; Jouini, M.; Chane Ching, K.I.; Lacaze, P.C., *Chem. Commun.*, 1998, 4, 489.
- [62] Lagrost, C.; Jouini, M.; Tanguy, J.; Aeiyaich, S.; Lacroix, J.C.; Chane-Ching, K.I.; Lacaze, P.C., *Electrochim. Acta*, 2001, 46, 3985.
- [63] Lagrost, C.; Chane-Ching, K.I.; Lacroix, J.C.; Aeiyaich, S.; Jouini, M., Lacaze, P.C.; Tanguy, J., *J. Mater. Chem.* 1999, 9, 2351.
- [64] Perruchot, C.; Hamady Hametou, M.J.; Dieng, M.M.; Koné, A.; Jouini, M., paper presented at EEM 2009, Szczyrk, Poland, July 14. – 19th, 2009, p. 38.
- [65] Vorotyntsev, M.A.; Aoki, K.; Heinze, J., *Russ. J. Electrochem.* 2003, 39, 182.
- [66] Vorotyntsev, M.A.; Heinze, J., *Electrochim. Acta*, 2001, 46, 3309.
- [67] Zotti, G.; Schiavon, G., *Synth. Met.*, 1989, 30, 151.
- [68] Brédas, J.L.; Scott, J.C.; Yakushi, K.; Street, G.B., *Phys. Rev. B*, 1984, 30, 1023.
- [69] Tourillon, G.; Garnier, F., *J. Phys. Chem.* 1983, 87, 2289.